Oxcarbazepine free or loaded PLGA nanoparticles as effective intranasal approach to control epileptic seizures in rodents

Teresa Musumeci; Maria Francesca Serapide; Rosalia Pellitteri; Alessandro Dalpiaz; Luca Ferraro; Roberta Dal Magro; Angela Bonaccorso; Claudia Carbone; Francisco Veiga; Giulio Sancini; Giovanni Puglisi

Abstract

The brain as a target for drug delivery is a challenge in pharmaceutical research. Among the several proposed strategies, the intranasal route represents a good strategy to deliver drugs to the brain. The goal of this study was to investigate the potential use of oxcarbazepine (OXC) to enhance brain targeting efficiency after intranasal (IN) administration. As well as attempting to use as low a dose as possible to obtain therapeutic effect. Our results showed that, after IN administrations, the dose of OXC that was effective in controlling epileptic seizures was 0.5 mg/kg (1 dose, every 20 min for 1 h) in rodents, confirmed by Cerebral Spinal Fluid (CSF) bioavailability. With the aim of reducing the number of administrations, sustaining drug release and increasing brain targeting, OXC was loaded into poly(lactide-*co*-glycolide) (PLGA) nanoparticles (NPs). The selected nanoformulation for *in vivo* studies was obtained re-suspending the freeze-dried and cryo-protected OXC loaded PLGA NPs. The translocation of 1-1′-Dioctadecyl-3,3,3′,3′-tetramethylindotricarbocyanine Iodide loaded PLGA NPs, from nose to the brain, was confirmed by Fluorescence Molecular Tomography, which also evidenced an accumulation of NPs in the brain after repeated IN administrations.

IN administrations of OXC loaded PLGA NPs reduced the number of administrations to 1 over 24 h compared to the free drug thus controlling seizures in rats. Immunohistochemical evaluations (anti-neurofilament, anti-beta tubulin, and anti-caspase3) demonstrated a neuroprotective effect of OXC PLGA NPs after 16 days of treatment. These encouraging results confirmed the possibility of developing a novel non-invasive nose to brain delivery system of OXC for the treatment of epilepsy.

Abbreviations

DiR
1-1′-dioctadecyl-3,3,3′,3′- tetramethylindotricarbocyanine Iodide
7n-PX
7-n-propylxanthine
AEDs
Antiepileptic Drugs
GFAP
anti-glial fibrillary acidic protein
BBB
blood brain barrier
BSA
bovine serum albumin
CBZ
carbamazepine

CNS
central nervous system
CSF
cerebral spinal fluid
DSC
differential scanning calorimetry
DMSO
dimetylsulfoxide
FDA
Food and Drug Administration
FT-IR
Fourier transform-infrared
Tg
glass transition temperature
HBHS
HEPES-Buffered Hanks Solution
HPLC
high performance liquid chromatography
IN
intranasal
IP
intraperitoneal
IV
intravenous
LOD
limit of detection
LOQ
limit of quantification
NPs
nanoparticles
NGS
normal goat serum
OXC
oxcarbazepine
PFA
paraformaldehyde
PTZ
pentylentetrazole
PBS
phosphate buffer solution
PCS
photon correlation spectroscopy
PDI
polidispersity index
RCS
Racine's Convulsion Scale
ROI
regions of interest
RSD
relative standard deviations
SEM

scanning electron microscopy
(ζ) or (ZP)
zeta potential

1. Introduction

As reported by the World Health Organization, it is estimated that about 50 million people worldwide suffer from epilepsy, correlated to the ageing population (http://www.who.int/en/news-room/fact-sheets/detail/epilepsy) [1], [2]. The control of seizures and the adverse effects of drug therapy represent relevant drawbacks for patients with epilepsy. In the European Forum on Epilepsy Research of 2013, which took place in Dublin, Ireland, the consultation of the different stakeholders highlighted several main concerns about epilepsy emergency, such as development of innovative biomarkers, therapeutic targets, and strategies paying attention to pediatric and aging populations [3]. The need for the development of innovative formulations to reach the brain, avoiding biodistribution, are the driving force to overcome limits associated with conventional drugs. Oxcarbazepine (OXC, or 10,11-dihydro-10-oxo-5H-dibenzazepin-5-carboxamide) is one of the new approved Antiepileptic Drugs (AEDs) [4]. It is a lipophilic compound approved as a first-line treatment for focal seizures with or without secondary generalization in epileptic adults and children [5]. In fact, in 2001, the European Medicine Agency approved Trieptal®, film-coated tablets containing OXC in three different dosage (150, 300, 600 mg) and the Food and Drug administration (FDA) approved the same dosage route and form named Oxtellar® in 2012. The use of this molecule protects against seizures and brain damage. OXC, derived from carbamazepine (CBZ), has a more favorable pharmacokinetic profile and an improved tolerability than CBZ, but it shows several secondary effects due to its high systemic distribution after oral administration that represents the widest dosage form [6].

The chance to treat patients with increased compliance and reduced side effects of common therapies is an important goal. In the last decade, intranasal (IN) administration of molecules has been an interesting approach to drug delivery to the brain overcoming blood brain limits of different exogenous molecules and increasing patients' compliance. The nasal route is attractive thanks to its non-invasiveness. There is increasing interest in direct nose to brain delivery because it is possible to avoid first-pass intestinal and liver metabolism and to decrease the dose of therapeutic substances. IN administration is patient friendly, low cost and safe and it is an alternative non-invasive method to bypass the blood brain barrier (BBB) and target drugs into the Central Nervous System (CNS). This goal is reached by the use of the appropriate device used to administer the substances in the cleft of the bulb region in the nasal cavity [7]. The major drawbacks associated with IN administration concern the mucociliary clearance and the small dose of active molecule that can effectively reach the brain. The drug concentration reaching the brain is sometimes lower than the therapeutic one because of the limited volume of the nasal cavity and the poor water solubility of AEDs resulting in poor absorption and insufficient therapeutic brain levels [8].

To overcome these limits different approaches have been proposed, for example Illum et al. described different absorption promoters and modulator absorption systems that could improve the dose into the brain [9]. As reported in different studies, biodegradable carriers have been used to carry drugs across the mucosal barrier and/or to protect the drugs from being degraded in the nasal cavity. Nanoparticles (NPs) are exciting systems for brain drug delivery because of the possibility to modulate them in terms of composition, shape, size, hydrophobicity, coating, chemistry, surface charge and ligands [10]. Considering the advantages and disadvantages of various approaches for drug delivery, the use of polymeric NPs is considered an interesting and promising tool [11], [12]. Among several types of polymeric NPs, nanosystems based on PLGA have been more attractive because of regulatory aspects (PLGA was approved by the FDA for human application) and

because of the physico-chemical and technological properties of the obtained nanocarriers. In our previous study, we demonstrated that, after IN administration, Rhodamine B loaded PLGA NPs reached the hippocampal region of the brain [13]. Taking into account that the hippocampus is a region affected by epilepsy, our previous finding encouraged us to explore the potential application of OXC loaded PLGA NPs.

In particular, our goal was to evaluate the potential administration of OXC through the IN route and the encapsulation of OXC in stable PLGA NPs aiming at direct nose to brain delivery to improve chronic anti-epileptic treatment in the rat. The nanosuspension was well characterized from the physico-chemical, morphological and technological point of view. *In vivo* fluorescence molecular tomography imaging was carried out with 1-1′-Dioctadecyl-3,3,3′,3′-tetramethylindotricarbocyanine Iodide (DiR) loaded PLGA NPs to investigate the translocation into the brain and into the body after single and repeated IN administrations in rodents. Behavioral and pharmacokinetic studies were performed because to detect the amount and the effect of free OXC in rats after IN administration. OXC loaded PLGA NPs were subsequently IN administered to evaluate the efficacy of a sustained release nanomedicine and of the neuroprotection effect of the drug against seizures and brain damage induced by pentylenetetrazole (PTZ) administration through behavioral tests and immunohistochemical analysis.

2. Material and methods

2.1. Material

OXC, Tween®80, 7-n-propylxanthine (7n-PX) and bovine serum albumin (BSA) were purchased from Sigma-Aldrich (Milan, Italy). Methanol, acetonitrile, ethyl acetate, and water were high performance liquid chromatography (HPLC) grade from Sigma-Aldrich. Male Wistar rats were purchased from Harlan SRC (Milan, Italy). All other chemicals were analytical grade, purchased from Analyticals, Carlo Erba. The polymer Resomer® 502H poly-(D, L-lactide-*co*-glycolide) (50:50) was purchased from Boehringer Ingelheim Pharma GmbH&Co. KG (Biberach, Germany). Ultrapure water was used throughout this study. DiR was purchased from Biotium (Fremont, California, USA).

2.2. Unloaded and OXC loaded PLGA nanoparticle preparation

Unloaded and OXC loaded PLGA NPs were prepared using the solvent displacement method followed by polymer deposition as previously reported [14]. Briefly, the chosen polymer (75 mg) was dissolved in acetone (20 mL). The organic phase was added, drop by drop, to 40 mL water/ethanol solution (1:1, v/v) containing 0.5% (w/v) Tween® 80 under magnetic stirring, obtaining a milky colloidal suspension. The organic solvent was then evaporated off under high vacuum at 40 °C. OXC loaded NPs were prepared by co-dissolving OXC (1% w/w drug/polymer) with the polymer in the organic phase. The different formulations were purified through ultracentrifugation (15,000*g*) for 1 h at 10 °C, using a Thermo Scientific SL16R centrifuge (ThermoFischer Scientific, Waltham, MA, USA) equipped with a thermofischer fiberlite F15-6x100y fixed-angle rotor. After washing, the obtained NPs were re-suspended in 5 mL of filtered water (0.22 µm Sartorius membrane filters). This procedure was repeated three times. The *in vivo* tested nanosuspensions were administrated after re-suspension of freeze-dried sample in the appropriate volume. Glucose at 5% w/V was added to the OXC loaded nanocarrier before the freeze-dried process to prevent instability of the formulation and to maintain the initial physico-chemical characteristics. The obtained samples were characterized according to size, size

distribution and surface, and then differential scanning calorimetry (DSC) and Fourier-transform infrared spectroscopy (FT-IR) were performed.

2.3. Characterization of OXC loaded PLGA nanoparticles

2.3.1. Differential scanning calorimetry analysis

Nanoparticles were sealed in an aluminum pan and submitted to DSC analysis to determine the incorporation of OXC in the NPs. A Mettler Toledo DSC 1 STARe system equipped with a PolyScience temperature controller (PolyScience Illinois, USA) was used to perform calorimetric analysis. The detection system was an HSS8 high sensitivity sensor (120 gold–gold/palladium-palladium thermocouples) and the ceramic sensor (Mettler Full Range; FRS5) with 56 thermocouples. The signal time constant was 18 s and the digital resolution of the measurement signal was less than 0.04 µW. Calorimetric resolution and sensitivity determined by TAWN test were respectively 0.12 and 11.9. The sampling rate was 50 values/s. The sensitivity was automatically chosen as the maximum possible by the calorimetric system, and the reference was an empty pan. The calorimetric system was calibrated, in temperature and enthalpy changes, by using indium by following the procedure of the DSC 1 Mettler TA STARe instrument. NPs were sealed in an aluminum pan and submitted to DSC analysis to determinate the influence of coating on the thermotropic parameters of the NPs. Each sample was submitted to heating and cooling cycles in the temperature range 20–250 °C at a scanning rate of 5 °C/min (heating) and at a scanning rate of 10 °C/min (cooling). Transition temperature was calculated from peak areas with Mettler STARe Evaluation software system (version 15.01) installed on an Optiplex 3020 DELL.

2.3.2. Particle size and zeta potential analysis

The particle size and the polidispersity index (P.D.I.) of nanoaggregates were performed by photon correlation spectroscopy (PCS) using a ZetasizerNano S90 (Malvern Instruments, Malvern, UK) at a detection angle of 90°, at 25 °C with a 4mW He-Ne laser operating at 633 nm. Each sample was measured in triplicate. The results are shown as mean ± standard deviation. The samples were analyzed using disposable cuvettes “DTS 0012 Disposable sizing cuvette”, withdrawing 700 µL of suspension. The zeta potential values (ZP), which reflect the electric charge on the particle surface, were determined at 25 °C using the same equipment describe previously. For the measurement, samples were diluted appropriately with ultra-purified water.

2.3.3. SEM analysis

Scanning electron microscopy (SEM) was performed to evaluate the surface morphology of NPs using a SEM Philips mod 500. NPs samples were dried for 24 h before the analysis. A small amount of NPs was stuck onto double-sided tape attached to a metallic sample stand, then coated, under argon atmosphere, with a thin layer of gold, using a POLARON E5100 SEM Coating Unit.

2.3.4. Fourier transform-infrared (FT-IR) analysis

FT-IR characterizations of PLGA, pure drug, physical mixtures and freeze-dried unloaded and drug-loaded NPs were performed using a FT-IR spectrophotometer (Perkin Elmer Spectrum RX I, USA) equipped with the Attenuated Total Reflectance (ATR) accessory (diamond/ZnSe). For each sample, 16 scans at a resolution of 2 cm^{-1} were obtained from a spectral range from 650 to 4000 cm^{-1}, using a speed of 0.50 cm/s and a force gauge of 100.

2.4. *In vivo* imaging

2.4.1. Preparation and characterization of DiR loaded NPs

Fluorescent loaded PLGA NPs were prepared with the same procedure reported above. In particular, DiR was added to the acetone (organic phase, 40 µg/ml). Fluorescent NPs were freeze-dried, after purification through centrifugation, to concentrate the final formulation. Accurate selection of the cryo-protectant (10% w/V, threalose) agent was carried out to maintain the particle size in the range suitable for nose to brain delivery.

2.4.2. Animals

All procedures involving animals and their care were conducted according to Italian law (DL 116/92) and policies, all protocols were approved by the Institutional Animal Care and Use Committee of the University of Milano-Bicocca. Male CD-1 mice, 6–8 weeks old, were purchased from Harlan Laboratories (Italy). They were housed in plastic cages, food and water were administered ad libitum and conventional conditions for laboratory animal care were respected (temperature 19–21 °C, humidity 40–70%, 12 h light/dark cycle). Mice were fed with chlorophyll-free food to avoid interference during fluorescence detection. Animals were anesthetized using a mixture of 2.5% isoflurane (Flurane) before treatment and during the whole fluorescence detection procedure.

2.4.3. Treatment schedule and polymeric nanoparticle biodistribution

Freeze-dried DiR-loaded PLGA NPs were re-suspended in 1 mL of sodium chloride physiologic solution and dispersed by sonication for 30 min at 25 °C, prior to *in vivo* administration. 20 µL of DiR-loaded PLGA NPs (37.5 mg/mL of PLGA, 10 µM of DiR) were instilled into the nose of mice, 10 µL in each nostril, with the help of a micropipette. The animals were held in a slanted position during IN administration to avoid swallowing NPs. Eight mice underwent a single IN instillation and the biodistribution of DiR-loaded NPs was analyzed 3, 24, 48 and 72 h after IN administration by means of a Fluorescence Molecular Tomography system (FMT1500, Perkin Elmer). An additional five mice were treated twice with DiR-labelled NPs by IN administration (24 h apart, 20 µL of NPs each time) and fluorescence was detected and quantified 3, 24, 48, 72 h after the second instillation. Regions of interest (ROI) were drawn in a blind manner and according to previously published data [15]. The total amount of fluorescence (in picomoles) of ROI was calculated by the provided TrueQuant software (Perkin Elmer) using previously generated standards of the appropriate dye.

2.5. *In vivo* OXC administration and quantification

2.5.1. Animals

Male Wistar rats (200–250 g; Charles-River S.r.l., Lecco, Italy) anesthetized (1.5% mixture of isoflurane and air) during the experimental period received a femoral intravenous infusion of 0.1 mg/mL OXC dissolved in a medium constituted by 20% (v/v) dimetylsulfoxide (DMSO) and 80% (v/v) physiologic solution, with a rate of 0.2 mL/min for 10 min. At the end of infusion and at fixed time points, blood samples (100 µL) were collected and CSF samples (50 µL) were withdrawn by the cysternal puncture method described by van den Berg et al. [16]. Briefly, before the experiments the rats were anesthetized and immobilized in a stereotaxic apparatus, after shaving off the skin overlying the neck. A needle connected to a syringe by means of polyethylene tubing and filled with sterile filtered water was attached to a holder on the stereotaxic frame. Following the appropriate stereotaxic coordinates, the needle was brought into position to carry out the puncture [17]. Before puncturing, an air bubble was drawn into the needle with a syringe at the other end of

the collection tubing. For puncturing, the needle was gently moved through the skin and muscles toward the cisterna magna. During needle placement, the syringe plunger was pulled back to create negative pressure; thereafter, the needle advancement was continued until the air bubble moved into the tubing followed by CSF. Then, the syringe and the tubing were disconnected from the CSF collection system and a Hamilton syringe was attached to the CSF collection tubing and used for CSF withdrawal. After sampling, the Hamilton syringe was disconnected and the tubing was closed with a clamp. Subsequent samples were taken by removing the clamp from the tubing, followed by attachment of the Hamilton syringe. This procedure requires a single needle stick and allows the collection of serial (40–50 µL) CSF samples which are virtually blood-free. A total volume of about 150 µL of CSF was collected during the experimental session. Considering that the total CSF volume in adult rats ranges from 300 to 400 µL, [18], [19] 50 µL of CSF should represent about 12% of the original total volume. Four rats were employed for femoral intravenous infusions. CSF samples (10 µL) were immediately injected into an HPLC system for OXC detection.

The blood samples were hemolyzed immediately after their collection with 500 µL of ice-cold water, and then 50 µL of 10% sulfosalicylic acid and 100 µL of internal standard (100 µM 7n-PX) were added. The samples were extracted twice with 1 mL of water-saturated ethyl acetate, and, after centrifugation, the organic layer was reduced to dryness under a nitrogen stream. One hundred and fifty microliters of a water–methanol mixture (50:50 v/v) was added, and, after centrifugation, 10 µL was injected into the HPLC system for OXC detection.

The *in vivo* half-life of OXC in the blood was calculated by nonlinear regression (exponential decay) of concentration values in the time range within 8 h after infusion and confirmed by linear regression of the log concentration values versus time.

IN administration of OXC was performed on anesthetized rats laid on their backs, by introducing 50 µL of a drug suspension (2 mg/ml) in a water/ethanol mixture (70:30 v/v) in each nostril of the rats using a semiautomatic pipet that was attached to a short polyethylene tube. The tubing was inserted approximately 0.6–0.7 cm into each nostril. After administration, blood (100 µL) and CSF samples (50 µL) were collected at fixed time points, and were analyzed with the same procedures described above.

All *in vivo* experiments were performed in accordance with the European Communities Council Directive of September 2010 (2010/63/EU), a revision of Directive 86/609/EEC, the Declaration of Helsinki, and the Guide for the Care and Use of Laboratory Animals as adopted and promulgated by the National Institutes of Health (Bethesda, Maryland, USA). The protocol of all the *in vivo* experiments was approved by the Local Ethics Committee (University of Ferrara, Ferrara, Italy). Efforts were mase to reduce the number of the animals and their suffering.

2.5.2. HPLC analysis

The quantification of OXC was performed by HPLC. The chromatographic apparatus consisted of a modular system (model LC-10 AD VD pump and model SPD-10A VP variable wavelength UV–Vis detector; Shimadzu, Kyoto, Japan) and an injection valve with 20 µL sample loop (model 7725; Rheodyne, IDEX, Torrance, CA, USA). Separations were performed at room temperature on a 5 µm Hypersil BDS C-18 column (150 mm × 4.6 mm i.d.; Alltech Italia Srl, Milan, Italy), equipped with a guard column packed with the same Hypersil material. Data acquisition and processing were accomplished with a personal computer using CLASS-VP Software, version 6.12 SP5 (Shimadzu Italia, Milan, Italy). The detector was set at 230 nm. The mobile phase consisted of a mixture of water and acetonitrile regulated by a gradient profile programmed as follows: isocratic elution with 10% (v/v) CH_3CN in H_2O for 5.5 min; then a 1 min linear gradient to 30% (v/v) CH_3CN in H_2O; the

mobile phase composition was finally maintained at 30% CH_3CN for 5.5 min. After each cycle the column was conditioned with 10% (v/v) CH_3CN in H_2O for 10 min. The flow rate was 1 mL/min. The xanthine derivative 7n-PX was used as internal standard for the analysis of rat blood extracts (see below). The retention times for 7n-PX and OXC were 4.9 and 11.8 min, respectively. The chromatographic precision, represented by relative standard deviations (RSD), was evaluated by repeated analysis ($n = 6$) of the same sample solution containing each of the examined compounds at a concentration of 25 μM. The solutes were dissolved in a 50:50 mixture of water and methanol (v/v). The RSD values ranged between 0.82% and 0.89% for the analyzed compounds. The calibration curve of peak areas versus concentration was generated in the range 1 to 100 μM of OXC and was linear ($n = 9$, $r = 0.997$, $P < 0.0001$). For CSF simulation, standard aliquots of balanced solution (phosphate buffer solution, PBS, Dulbecco's medium without calcium and magnesium) in the presence of 0.45 mg/mL BSA were employed [19]. In this case, the chromatographic precision was evaluated by repeated analysis ($n = 6$) of the same sample solution containing 1.0 μM OXC whose RSD value was 0.91% and calibration curve of peak areas versus concentration was generated in the range 0.1 to 10 μM (corresponding to 0.025 to 2.52 μg/ml), resulting linear ($n = 8$, $r = 0.993$, $P < 0.0001$). The limit of quantification (LOQ) at a signal-to-noise ratio of 10 for OXC dissolved in the CSF simulation fluid was 270 nM (68 ng/ml; 0.68 ng injected) whereas the limit of detection (LOD) at a signal-to-noise ratio of 3 was 81 nM (15 ng/ml; 0.15 ng injected). The accuracy of the analytical method for OXC extracted from rat whole blood was determined by comparing the peak areas of 40 μM OXC (corresponding to 10.09 μg/ml) extracted at 4 °C ($n = 3$) with those obtained by injection of an equivalent concentration of the analyte dissolved in the water-methanol mixture (50:50 v/v). The average recovery from rat whole blood ± S.E. was 96 ± 3%. The concentrations of OXC were therefore referred to as peak area ratio with respect to the internal standard 7n-PX. The precision of this peak area ratio-based method is demonstrated by the RSD values of 1.06% for 40 μM OXC extracted from rat blood at 4 °C, whose calibration curve was linear over the range 0.8–100 μM (corresponding to 0.2 to 25.23 μg/ml; $n = 9$, $r > 0.991$, $P < 0.0001$). The LOQ at a signal-to-noise ratio of 10 for carbamazepine extracted from rat whole blood was 640 nM (160 ng/ml; 1.6 ng injected); the LOD at a signal-to-noise ratio of 3 was 190 nM (49 ng/ml; 0.49 ng injected).

2.6. *In vivo* treatment of OXC free and loaded NPs on rats treated with PTZ induced seizures

All the experiments were performed following the Guidelines for Animal Care and Use of the National Institutes of Health. The study was approved by Italian Ministry of Health (permit number 183). Thirty-three male rats (Wistar strain, Harlan) weighing 200–220 g were acclimatized for one week before the study, with free access to water and food. They were divided into seven groups. The animals were lightly anaesthetized with Zoletil 100 (100 mg/kg, i.p.) and placed on a heated working surface to prevent hypothermia. The first lot of animals (10 rats) received a single intraperitoneal injection of PTZ dissolved in 0.9% saline solution at different concentrations (75, 58, 50, 42 and 30 mg/kg w.b.). The minimum effective dose was found to be 50 mg/kg w.b. Following the PTZ injections, the animals were placed in clear plexiglass boxes for observation of seizure activity and observed for 30–60 min [20] as well as the evaluation of Racine's Convulsion Scale (RCS, 1972). Briefly, stage-1 mouth movements and facial twitches, stage-2 head nodding, stage-3 forelimb clonus, stage-4 clonus and rearing, stage-5 clonus, rearing, jumping and falling on the back.

The second lot of animals (8 rats) received a single IN administration of free OXC at different concentrations (0.2, 0.4, 0.5, 0.8 mg/kg w.b.) dissolved in 100 or 50 μL of saline solution and ethanol (1:1). The effective dose was found to be 0.5 mg/kg w.b. The IN instillation was given according to Dyer et al. [21]. Briefly, the rats were placed in a supine position and 25 μL were

administered in each nostril using a microliter syringe attached, via a needle, to a short polyethylene tube, inserted approximately 0.7 cm into each nostril. The procedure was performed slowly in about 1–2 min. The third lot of animals (three rats) received a single IN administration of 50 µL of OXC (0.5 mg/kg) loaded PLGA NPs. The fourth lot of animals (three rats) received a single IN administration of 50 µL of unloaded PLGA NPs. The fifth, sixth and seventh lots of animals (three rats for each lot) received three, eleven and sixteen IN administrations (one every 24 h) of 50 µL of OXC (0.5 mg/kg) loaded PLGA NPs, respectively. Thirty minutes after the last free OXC or loaded PLGA NPs administration, all rats from the second to the seventh lot received a single PTZ injection and the efficacy against seizures was observed for 2 h.

Twenty-four hours after PTZ injection, all the rats were deeply anesthetized by i.p. injection of Zoletil 100 (100 mg/kg) and Dexdomitor (20–30 µg/Kg) and perfused trancardially with 4% paraformaldehyde (PFA) solution in 0.1 M phosphate buffer (pH 7.4). The brains were removed, post-fixed overnight in the same 4% PFA and then transferred into a 30% sucrose in PBS as cryo-protective solution at 4 °C for 2–3 days. Serial 25 µm frozen sections of the brains were cut in the sagittal plane and subjected to immunohistochemical assay. Briefly, free-floating sections were washed three times in PBS and then blocked at room temperature for 1 h in 5% normal goat serum (NGS) in PBS. They were then incubated overnight at 4 °C with the following antibodies: rabbit polyclonal anti-caspase (1:200, Abcam) as apoptotic marker; anti-Glial Fibrillary Acid Proteic (GFAP, 1:400 DAKO) as astroglial marker; mouse monoclonal anti-NeuroFilament (NF 1:200, Abcam) and anti-Tubulin (1: 400 Sigma-Aldrich, Milan, Italy) as neuronal markers. All the antibodies were diluted in a PBS solution with 1% NGS and 0.01% Triton X-100. The sections were then rinsed in PBS and incubated in secondary antibodies diluted in PBS plus 1% NGS and 0.01%Triton X-100. The secondary antibodies were: goat anti-rabbit antibody IgG Fluorescein Isothiocyanate (FITC, 1:200; Immunological Research) to visualize the caspase-3 and GFAP positivity, and Cy3 anti-rabbit antibody (1:200; Jackson ImmunoResearch, Laboratories, Inc) to visualize NF and Tubulin (TUB) positivity.

The sections were examined under a fluorescence microscope (Nikon Eclipse 80i) equipped with filters for the visualization of Cy3 (550–570 nm wavelength) and FITC (450–520 nm wavelength). Images were captured using a digital camera (Nikon) and adjusted for contrast with Adobe Photoshop without compromising data integrity. No non-specific staining of cells was observed in control incubations in which the primary antibodies were omitted.

2.7. Statistical analysis

Statistical analysis was performed using Prism 6 (GraphPad Software, Inc., La Jolla, CA, USA). Results are expressed as mean ± SD. Statistical analysis used one-way analysis of variance (ANOVA) followed by Student's *t* test for the biodistribution study of DiR PLGA NPs; Dunnett's test for dose-curve and behavioral studies. Significance was defined as $p < 0.05$.

3. Results and discussion

Nanoparticles based on biocompatible and biodegradable polymers approved by the FDA and EMA (European Medicines Agency) represent a relevant effort in nanomedicine. In particular, PLGA polymers are a widely used material to develop nanosystems for different administration routes [22].

As regards the intranasal route, the most used polymers are chitosan or PLGA-PEG polymers because of their mucoadhesive properties that allowed increased residence time at the local site [21], [23], [24], [25], [26].

Currently, two main theories are being investigated and debated regarding brain targeting by IN administration. The first explains brain targeting as a combination of different pathways sustaining the drug that reaches the brain: olfactory or systemic routes [27], [28]. The second takes into account the direct access of NPs to the brain along olfactory axons or by transcellular mechanisms in the olfactory region [29], [30]. In our previous work, Bonaccorso et al. [13], showed that fluorescent NPs with a positive charge (chitosan coated PLGA NPs) showed a delay in reaching the brain and prevalently accumulated in the caudal region of the rat brain within 24 h from IN administration. Our study cannot exclude systemic pathway involvement. For this reason, we were encouraged to explore the potential application of PLGA nanoformulation for loading OXC by IN delivery.

3.1. Physico-chemical characterization of optimized unloaded and OXC loaded PLGA NPs

Here we present the characterization of our selected nano formulation obtained by optimization of different parameters for long-term storage nanoformulation with physic-chemical properties suitable for nose to brain delivery.

OXC loaded PLGANPs were obtained by nanoprecipitation, which is a simple and reproducible method used for encapsulation of hydrophobic compounds in these polymers. The method is easy to perform, giving the instantaneous formation of NPs in a colloidal suspension [25]. In this study, the nanoprecipitation method was successfully applied to obtain OXC PLGA NPs with a mean diameter of about 250 nm and a good homogeneity (PDI < 0.15) after the re-suspension of freeze-dried powder (Table 1).

Table 1. Z-average hydrodynamic diameter, zeta potential, polydispersity index (PDI), and encapsulation efficiency (EE%) data for the various re-suspended freeze-dried nanoformulations.

Formulations after freeze-dried process	Size (nm) (±SD)	Zeta potential (ζ) (±SD)	PDI (±SD)	EE% (±SD)
Unloaded PLGA NPs with glucose as cryo-protectant	212.56 ± 5.45	−16.81 ± 0.42	0.093 ± 0.031	–
OXC loaded PLGA NPs with glucose as cryo-protectant	256.16 ± 2.94	−15.12 ± 0.36	0.144 ± 0.024	85.1 ± 2.1
OXC loaded PLGA NPs with glucose as cryo-protectant storage 24 months	294.2 ± 10.39	−14.23 ± 2.39	0.289 ± 0.090	83.4 ± 3.2
DiR loaded PLGA NPs with 10 µM threalose as cryo-protectant	336.5 ± 5.6	−12.45 ± 3.3	0.330 ± 0.056	5.1 ± 0.8

Abbreviations: PLGA, poly(lactic-*co*-glycolic acid); SD, standard deviation.

It has been widely demonstrated that colloidal carriers are instable in aqueous media for long-term storage [31], [32]. To achieve this a freeze-drying process is performed both to increase stability and to concentrate the nanosuspension. This procedure produces alteration of physic-chemical parameters (size, homogeneity) of NPs without the use of an appropriate cryo-protectant agent added before the freeze-drying process.

For our goal a controlled size and homogeneity is important to obtain a translocation of NPs from the site of administration (nose) to the target (brain). In fact, as demonstrated by Mistry et al. [33], the size of NPs influenced uptake mechanisms in excised porcine olfactory epithelium and

consequently the fate of NPs with their cargo. Thus, glucose was used in the formulations loaded with OXC as a cryo-protectant to shield OXC loaded PLGA NPs from freezing stress and to increase their stability during storage. Type and concentrations of the cryo-protectant, glucose, were chosen based on the results obtained in our previous study that showed its efficacy also with OXC loaded NPs [34]. The most useful cryo-protectants are sugars because they affect the glass transition temperature (Tg) resulting in a freeze-dried cake with a stable amorphous form, a high redispersion speed, and stabilization during long-term storage. Glucose vitrifies at a specific temperature denoted (Tg). The immobilization of NPs within a glassy matrix of cryo-protectant can prevent their aggregation and protect them against the mechanical stress of ice crystals [25], [31].

OXC loaded PLGA NPs were negatively charged and did not significantly change between unloaded and loaded OXC PLGA NPs. It is possible to obtain this result when OXC is well incorporated within the polymeric network. In addition, the slight increase in average size of NPs demonstrates the presence of OXC in the inner core of the nanocarrier. Formulation homogeneity was maintained as revealed by the PDI value (0.144 ± 0.024) as well as PLGA NP stability. We performed physico-chemical characterization after 24 months of storage; the sample was screened for its size and surface properties. As reported in Table 1 NP mean size increased from 256.16 nm to 294.2 nm, which can be considered not very relevant for our purpose, whereas surface charge and PDI only slightly changed. The formulation was stable after 2 years of storage as freeze-dried powder, no variation in terms of size, surface charge or encapsulation efficiency was found after re-suspension.

The scanning electron microscope images showed that the OXC loaded PLGA NP formulation appeared to be uniform with almost smooth and spherical shape (Fig. 1 supplementary data). As reported in Table 1 this formulation presented a high EE % (85.1 ± 2.1) which was, once more, maintained after 2 years of storage. All together, these values showed that OXC is well located in the NP structure, even after long-term storage, suggesting that it is a promising formulation for intranasal administration. OXC was released from PLGA NPs in prolonged and sustained profile until 72 h (Fig. 2 supplementary data), without any burst effect.

3.2. Fourier transform-infrared (FT-IR) analysis and thermal analysis of OXC loaded PLGA NPs

Fourier-transform infrared spectroscopy (FT-IR) gives information about the groups present in the structure of a material and the occurrence of chemical interactions. IR spectrum of OXC, PLGA, their physical mixture, freeze-dried unloaded and OXC-loaded NPs were obtained (Fig. 1A).

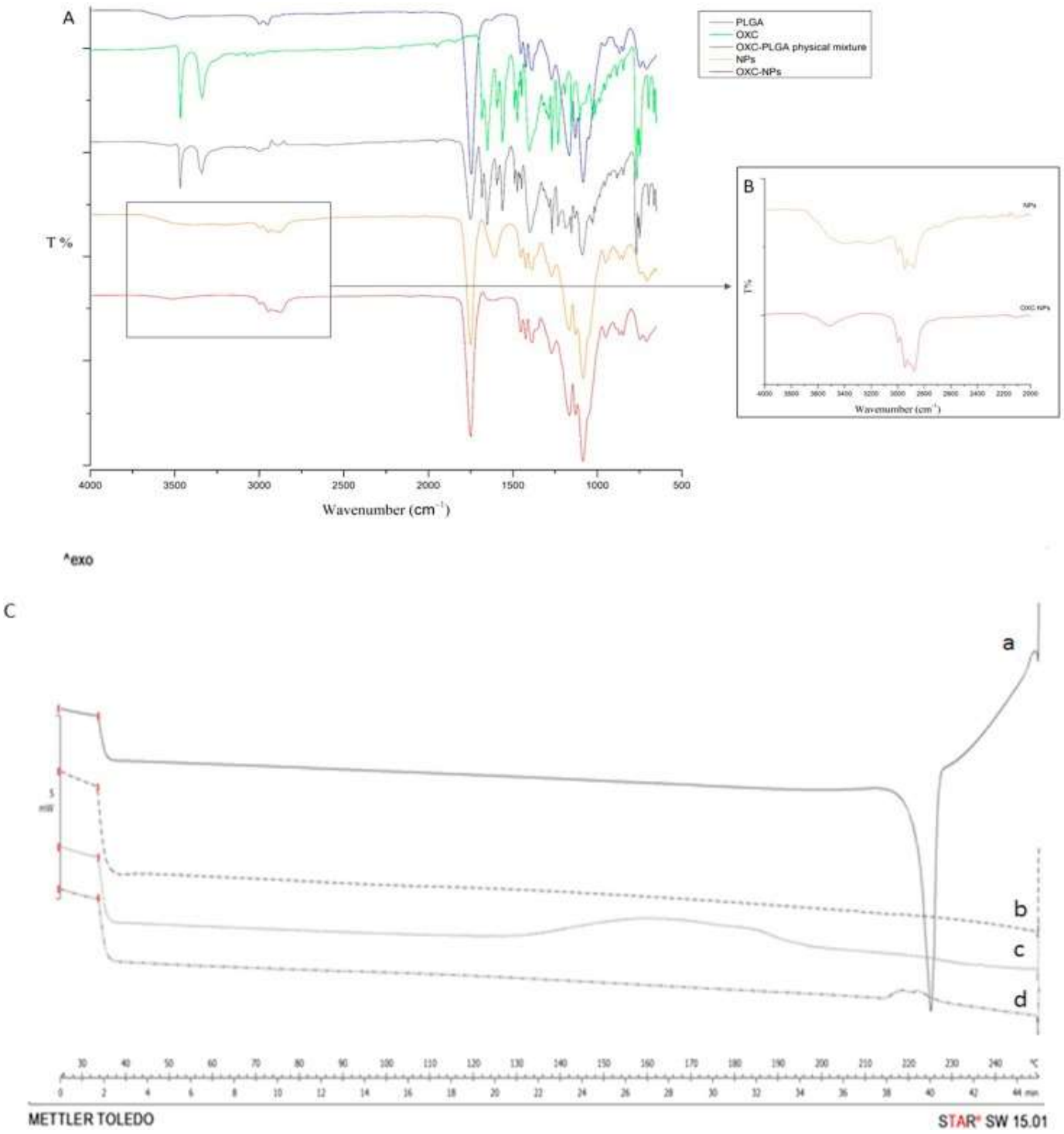

Fig. 1. IR Specta of: PLGA, pure OXC, their physical mixtures and freeze-dried unloaded and OXC-loaded NPs (A). Enlargement of IR spectrum of unloaded NPs and OXC-loaded PLGA NPs (B). DSC thermograms (C) of OXC (a), PLGA (b), unloaded NPs (c) and OXC loaded PLGA NPs (d).

Different peaks in IR spectra were interpreted for the presence of different groups. According to literature data, the IR spectrum of PLGA, as raw material, shows the characteristic peak at 1745 cm^{-1} (carbonyl CO stretch), as well as peaks in the range 1000–1170 cm^{-1} (CO stretch), peaks in the range 2949 and 2997 cm^{-1} (CH, CH_2 and CH_3 stretching vibrations), and OH stretching around 3500 cm−1 [35]. FT-IR spectrum of OXC shows that the drug is in a crystalline form and the characteristic drug peaks are shown at 3466.55 cm^{-1} and 3339.34 cm^{-1} [36]. The physical mixture

shows the presence of the main peaks of both the polymer and the drug, thus confirming the absence of chemical interaction between the two compounds (Fig. 1 panel A). The IR spectrum of unloaded NPs clearly shows the same peaks of the pure polymer, confirming that the main structure of PLGA does not change with the increase of CO strength as revealed by the increasing intensity of the peak at 1608 cm^{-1}. The spectrum of OXC-loaded PLGA NPs exhibited the same characteristic peaks of unloaded NPs, except for the decrease of the intensity of the carbonyl stretch together with a slight shift of OH stretching (3511 cm^{-1}) (Fig. 1B). According to literature, a slight shift or modification in the intensity of the peaks is related to the possible overlapping between the characteristic polymer and drug peaks [27]. Based on this consideration, the FT-IR spectra indirectly suggested the occurrence of a slight drug-polymer interaction, thus confirming that the drug was successfully encapsulated in PLGA NPs.

According to FT-IR results, DSC was performed to confirm OXC entrapment in NPs. As can be seen in Fig. 1C, the DSC curve of OXC (a) shows an endotherm with a melting point at 226 °C at a rate of 5 °C per min due to its crystalline nature. Moreover the exothermic peak reported in curve (d, between 215 and 225 °C) should be related to a drug decomposition phenomenon as reported by Lutker and Matzger which is concomitant with the melt [37]. No distinct melting point was observed in thermograms (b) and (c) because PLGA is amorphous in nature. The OXC endothermic peak disappears in thermogram (d) suggesting the effective incorporation of the drug in the PLGA-NP system. Hence, it could be concluded that in the prepared PLGA NPs the drug was present in the amorphous phase and may have been homogeneously dispersed in the PLGA matrix. The DSC study did not detect any crystalline drug material in the OXC-loaded PLGA NP sample, as the sharp peak of the drug was absent. Thus, the drug incorporated in the NPs was in an amorphous or disordered-crystalline phase of molecular dispersion or solid solution state within the polymer matrix [38].

3.3. The fate of fluorescent NPs through *in vivo* fluorescence molecular tomography imaging

With the aim of confirming our previous results that clearly demonstrated the brain distribution of Rhodamine B labeled PLGA NPs and Chitosan-PLGA NPs [13], further distribution studies were performed. In particular, PLGA NPs were loaded with carbocyanine DiOC18(7) (DiR). Biodistribution and bioavailability to the brain was evaluated after IN administration in healthy mice by Fluorescence Molecular Tomography (FMT) [39], [40] (Fig. 2). DiR-loaded PLGA NPs were prepared by the nanoprecipitation method by co-dissolving the DiR dye with the polymer in the organic phase [14]. DiR-PLGA NPs were purified by ultracentrifugation, then, after washing, the obtained NPs were re-suspended in filtered water (0.22 μm Sartorius membrane filters) and freeze-dried using trehalose as the cryo-protective agent. The use of glucose or trehalose as the cryo-protective agent for the same nanoparticle system is justified by the presence of different compounds encapsulated within the polymeric matrix. As revealed by our experimental data (data not published), the presence of a specific molecule in the inner core and/or outer shell of the nano system affects the efficacy of the cryo-protectant leading to a homogeneous re-dispersion of the lyophilized powder or in large and heterogenous aggregates. In a first step of our study, we proposed glucose, but the re-suspended powder did not give the desired results (data not reported). We carried out an optimization study to determine the appropriate cryo-protectant agent as well as the amount to use to stabilize the nano suspension in the appropriate range for nose to brain delivery. The use of trehalose before the freeze-drying process allowed us to obtain a stable and concentrated formulation that could be easily re-suspended in a specific small volume; this is a crucial point as volume is one of the biggest limitations for IN dosing. DiR-loaded PLGA NPs were characterized for ζ potential and size distribution by PCS (Table1). DiR-loaded PLGA NPs with an average diameter of 336.5 ± 5.6 were obtained having a polydispersity index of 0.330 ± 0.056. This

formulation was negatively charged and with a DiR concentration of ~10 μM. Freeze-dried DiR-loaded NPs were re-suspended in 1 mL of sodium chloride physiologic solution and dispersed by sonication for 30 min at 25 °C prior to *in vivo* administration.

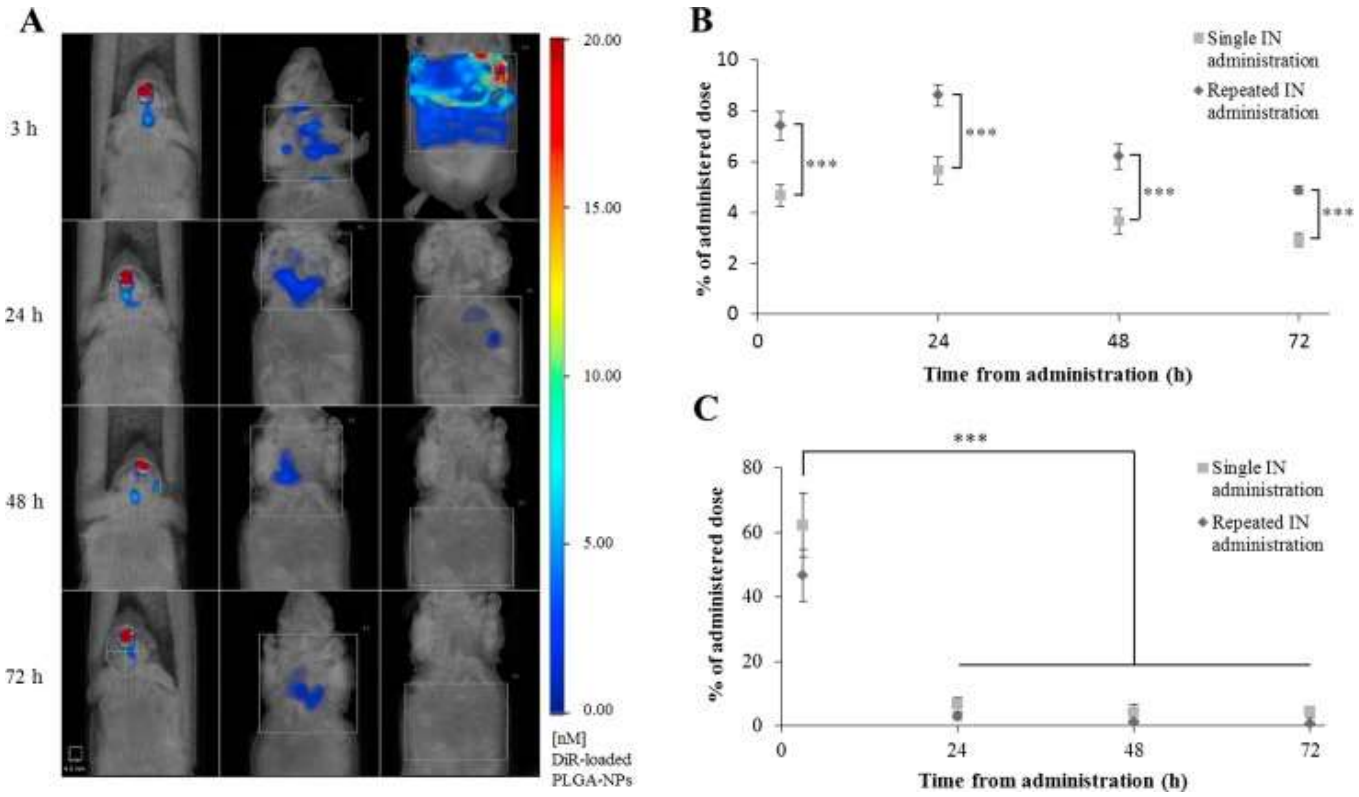

Fig. 2. DiR-loaded PLGA NPs biodistribution and biovailability in the brain. Representative image of DiR-loaded PLGA NP biodistribution in mice at different times after the second IN administration. Fluorescence was detected by a FMT1500 and the amount of fluorophore (DiR) in the regions of interest (ROI) was quantified using TrueQuant Software (A). Quantification of fluorescence associated with DiR loaded PLGA NPs in the brain (B) and body (C) of CD-1 mice after single and repeated IN administrations. Values of repeated IN administrations are related to the % of fluorescence measured in the brain 3, 24, 48 and 72 h after the second instillation. Data are expressed as % of the instilled NPs. $^{***}p < 0.001$ by Student's *t* test (B).

Our results showed that 3 h after a single IN administration, more than 5% of the instilled dose of the NPs was detectable in the brain (Fig. 2A and B). Repeated IN administrations provided a significant increase of NP-associated fluorescence in the brain. Indeed, more than 8% of the instilled DiR-loaded PLGA NPs was measured in the brain 24 h after the second IN instillation. This amount slowly decreased to 4.9% at 72 h from the last IN administration. Repeated IN administrations did not affect NP accumulation in other organs and tissues (Fig. 2C). NPs were quickly cleared from the thorax and from the abdominal cavity. Less than 10% of the instilled dose was found in extracerebral organs 24 h after a single and repeated instillations (data not reported). These findings support a proof of concept for the translocation of PLGA NPs from nose to brain bypassing the blood brain barrier, according to our previous results on Rhodamine B loaded NPs [13]. Here, we confirm again the translocation of PLGA NPs from the nasal cavity to the brain after IN administration. We cannot exclude a possible role for the systemic pathway involved in this transport, through nasal mucosa, but we believe that the neural pathways are predominant.

3.4. Behavioral study and pharmacokinetic profile of IN OXC in rats

To the best of our knowledge, experimental evidence of efficacy of OXC has not been reported after IN administration. Fortuna et al. (2014), who showed a drastic reduction of efficacy dose when administered intranasally, studied free carbamazepine [41]. To evaluate the potential use of OXC for IN administration and to determine the dose that should be entrapped in NPs, first we carried out a study to determine the dose-response curve of OXC intranasally administrated in rodents treated with a single IP-PTZ injection, as an animal model of epileptic seizures. Rats were treated with different PTZ doses to select the concentration that induced epileptic seizures. Thanks to this preliminary evaluation 50 mg/kg was the concentration of PTZ selected. At the highest dose of PTZ (75 mg/kg and 58 mg/kg of PTZ) all the animals were dead after a few minutes, instead, lower concentrations of PTZ (42/Kg and 30 mg/kg) caused only mild symptoms without convulsions (Fig. 3A). Therefore, we selected 50 mg/kg PTZ as the concentration to use for our studies because this dose induced the characteristic signs of epileptic discharge such as persistent generalized tonic clonic seizure but not death.

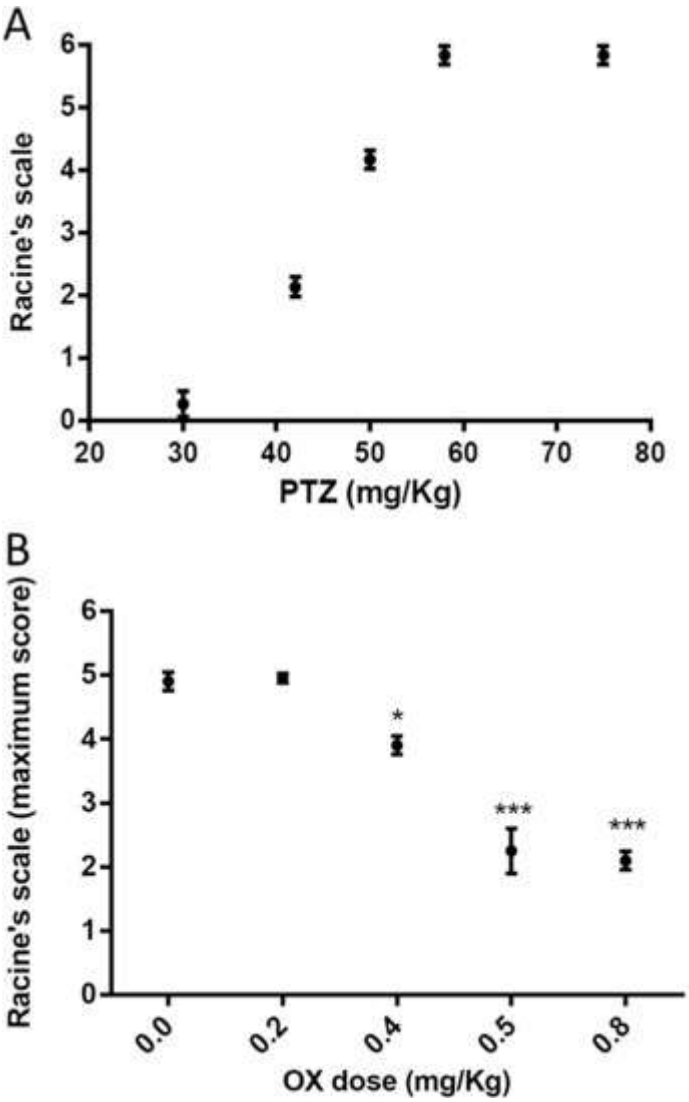

Fig. 3. Rats were treated with different doses of PTZ, monitored for observable seizures, and classified on the Racine Scale (A). Values are presented as the mean ± S.D. (n = 3). Racine's Dose-Response scale at different doses (0.2, 0.4, 0.5, 0.8 mg/kg) of free OXC after IN administration in an animal model of epileptic seizures induced by PTZ in rats. Dunnett's test for dose-curve and behavioral study. Significance was defined as $p < 0.05$ (B).

We performed behavioral tests to evaluate the seizure control after free OXC administered through the nasal route at different doses (from 0.2 to 0.8 mg/kg) and 30 min after the last administrated dose we induced seizures by 50 mg/kg of PTZ. The rats were observed for 60 min after PTZ injection for the evaluation of RCS. To detect some effects, multi-doses of OXC were administered. No significant differences were observed between animals treated with 0.5 and 0.8 mg/kg of the drug (Fig. 3B). Therefore, our results demonstrated that the minimum concentration of OXC required to produce a protective effect against seizures was multiple IN administration (1 dose, every 20 min for 1 h, total doses: 3) of 0.5 mg/kg.

Furthermore, the same dose administrated IP (0.5 and 0.8 mg/kg) failed to control symptoms induced by PTZ (data not shown), according to Hainzl et al. [42] who used 20 mg/kg IP to control seizures in rats. This result is a very interesting piece of experimental evidence that supports the use of OXC free drug intranasally at lower dosages with respect to the IP dosage. Behavioral results are in agreement with our pharmacokinetic study. In order to investigate the potential applicability of the nasal route for the administration of free OXC and to confirm our behavioral findings, we studied the pharmacokinetics profiles of OXC in CSF and in the blood of rats after IN and IV administrations.

We employed a water/ethanol 70:30 v/v suspension of the free drug for the nasal administration of pure OXC as a suspension, the low dose administrated for the quantitative study was selected from the results of the behavioral study. As shown in Fig. 4, OXC as free molecule produced detectable amounts of OXC in the CSF of the rats after IN administration.

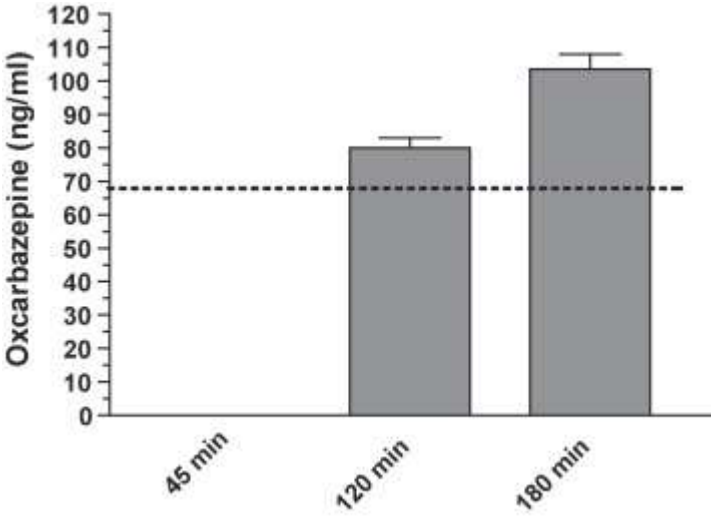

Fig. 4. Oxcarbazepine concentrations (ng/mL) detected until 180 min in the CSF after IN administration of 1 mg/kg of the drug suspended in a water/ethanol mixture (70:30 v/v). The dashed line reports the limit of quantification (LOQ) of OXC. Data are expressed as the mean ± SD of four independent experiments.

In particular, the analysis of CSF samples indicated that OXC was below its limit of quantification (LOQ, 68 ng/ml), so very poorly detectable 45 min after the nasal administration of the suspension, whereas after 120 and 180 min the drug amounts detected were 80 ± 3 and 104 ± 4 ng/ml, respectively. No OXC amounts were detected in the bloodstream within 180 min after nasal administration of the drug suspension. These results suggest a direct nose to CNS transfer of OXC due to its rapid appearance in the CSF and its simultaneous absence in the bloodstream. Therefore it seems unlikely, at least for this specific dose, a plasma-to-CSF transfer of OXC across the choroid plexus which form the blood–cerebrospinal fluid barrier (BCSFB) [43]. OXC, as a free drug, is able

to reach the brain by means of IN administration without the help of absorption promoters or specific formulations such as micro- and/or nano-particles.

When the same dose was administered by intravenous (IV) infusion a different trend was observed, as shown in Supplementary Fig. 3 (supplementary data), which shows the blood OXC concentrations detected in rats after IV infusion of the free drug. The peak concentration obtained at the end of the IV administration was 15.16 ± 0.54 μg/ml and was decrease over time (8 h) with an apparent first order kinetic confirmed by the linearity of the semi-logarithmic plot shown in the inset of Supplementary Fig. 3 ($n = 9$, $r = 0.980$, $P < 0.0001$), and a half-life of 3.23 ± 0.24 h. No OXC amounts were detected in the CSF within 180 min after IV administration of the drug.

Comparing our results with another scientific study, the dose required after IV administration for OXC to reach the brain from the blood is higher than 0.5 mg/kg, in particular, ranging from 20 to 200 times more, as previously demonstrated by Clinckers et al. [44]. Moreover, as a further support of our experimental result OXC was recognized to be a substrate for active efflux transporters (such as P-gp and MRP) at the BBB [2].

The present pharmacokinetic findings demonstrated that free OXC can reach the brain after IN administration, although at low concentrations. From a pharmacological point of view, by itself this finding does not doubtless demonstrate the advantage of IN OXC over other drug administration routes. In fact, following its oral or IV administration, OXC is extensively reduced by cytosolic enzymes in the liver to its pharmacologically active 10-monohydroxy metabolite (MHD) [45].

Based on this evidence, it would be also relevant to compare the CSF concentration of MHD after intranasal and IV administration. However, it is outside the scope of the present pharmacokinetic study simply aimed at evaluating whether and in which extent OXC can reach the brain after IN administration, to provide a rationale for the development of OXC loaded NPs to be tested for their efficacy in an animal model of epileptic seizures (*see below*). The relevance of this approach is also supported by the evidence that OXC and MHD exhibit comparable antiepileptic efficacy [6].

Thus, after OXC oral administration the pharmacological action of the drug is mainly attributable to MHD.

Thus, taking into account all the findings obtained by pharmacokinetic and behavioral studies, we can deduce that very low amount of free OXC can reach the CNS after the IN administration. In order to achieve the effective OXC dose in the brain, higher concentrations of the drug or multiple administrations are required daily. It is important to notice that less frequent dosing regimens resulted in better patient compliance, especially during chronic therapy. Thus, the drug entrapment in the controlled release nanosuspension is a convenient strategy to increase compliance and improve the drug concentration in the brain.

3.5. Evaluation of the effect of OXC loaded NPs after repeated IN administrations on seizures induced in rodents

With the aim of reducing the number of administrations and improving OXC translocation from the nose to the brain, the drug was encapsulated in PLGA NPs. Behavioral studies and immunohistochemical analyses were performed to evaluate the efficacy of the treatment after IN administration of nanosuspensions. Based on the data reported in our previous study, the dose of OXC loaded PLGA NPs was given daily, in fact, we showed that rhodamine B loaded PLGA NPs present an intense labelling in the hippocampus 24 h after nasal instillation [13].

Thus, 0.5 mg/kg of OXC loaded PLGA-NPs were administered once daily for 3, 11, and 16 days. The day after the last administration, PTZ (50 mg/kg) was injected and rats were observed for 60 min to evaluate RCS. OXC loaded PLGA NPs significantly reduced the appearance of symptoms and their duration after intranasal administration. Briefly, summing up the results obtained so far, OXC given intraperitoneally failed to induce protection; OXC given intranasally (0.5 mg/kg) with multiple administrations offered prolongation of the onset of PTZ-induced seizures, reduction in seizure stage and symptom duration. This partial protection is may be due to the limited ability of the IN solution to deliver the drug in suitable concentrations to the brain. After OXC-NP (0.5 mg/kg) administration intranasally once daily for 3 days, rats did not show any symptoms related to first stage seizures. These results support our published data, where we speculated that PLGA NPs reach the hippocampus region after 24 h and the prevalent pathway involved is olfactory [13].

In order to establish if OXC exerts protection against brain cell damaged by PTZ we performed immunohistochemical analysis. We choose the CA1–CA3 regions and the granular layer of the dentate gyrus of the hippocampus because it is very involved during seizures. Fig. 5 shows the immunopositivity of the GFAP in the hippocampus area in controls, after PTZ administration and after daily intranasal administrations of OXC loaded NPs for 3–11–16 days. It is worth noting that after PTZ injection and 3-days of administrations of OXC in NPs, a high GFAP-positivity was found indicating a strong gliosis, with respect to controls. This result demonstrates that 3 daily administrations of OXC in NPs failed to induce protection; even if in the experimental animals, the number and the signs of convulsive episodes were decreased compared with controls (animals receiving PTZ alone).

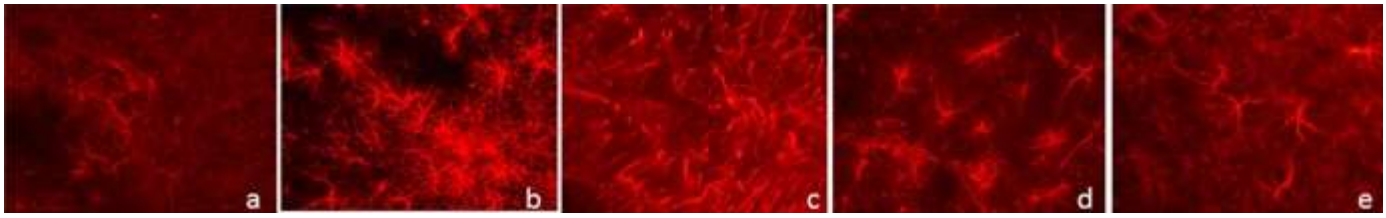

Fig. 5. Photomicrographs illustrating the expression of anti-glial fibrillary acidic protein (GFAP) in the hippocampus after repeated PTZ-OXC loaded PLGA NP IN administration at different days of treatment. Positive Control (a); PTZ-negative control (b). OXC loaded PLGA NPs: 3 (c); 11 (d) and 16 (e) days. Scale bar = 50 μm.

Therefore, we chose to extend the administration of OXC loaded NPs for 11 and 16 days. In these animals, the behavioral analysis showed the absence of generalized seizures and only a few symptoms typical of the 1st–2nd stages of Racine's scale (Table 2). These results were further confirmed by the immunohistochemical study.

Table 2. Seizure scores after intranasal administrations of free or OXC loaded nanoformulation (once daily) in rodents, tested dose of loaded OXC 0.5 mg/kg.

Treatment	Time of treatment (days)	Seizure score
PTZ (negative control)	–	4.83 ± 0.16
PTZ + OXC (positive control)	0.08 (2 h)	2.92 ± 0.06**
PTZ + OXCPLGA NP	1	4.02 ± 0.57***
PTZ + OXCPLGANP	3	2.01 ± 0.01***
PTZ + OXCPLGANP	11	2.10 ± 0.05***

Treatment	Time of treatment (days)	Seizure score
PTZ + OXCPLGANP	16	2.05 ± 0.03***

PTZ: pentylenetetrazole (50 mg/kg, i.p); OXC: oxcarbazepine (IN). Values are expressed as mean SEM, n = 5 in each group; Statistical analysis was performed using analysis of variance (ANOVA) followed by Dunnett's test. A $p < 0.05$ was taken as level of significance.

**

$p < 0.01$.

***

$p < 0.001$.

To verify if gliosis is present after PTZ and PTZ-OXC administration we labeled the sections of the hippocampus with GFAP, which was used to identify reactive astrocytes. In Fig. 5 a very light labeling is seen in the control rats (Fig. 5a); increased expression levels of GFAP were observed after PTZ administration when compared with the control rats (Fig. 5b). In the rats with multiple OXC administrations followed by PTZ injection, we detected a progressive decrease of expression levels of GFAP in a dose-dependent manner in rats treated with OXC for 3 (Fig. 5c), 11 (Fig. 5d); and 16 (Fig. 5e) days, when compared with rats treated only with PTZ. These data demonstrated that multiple OXC administrations could reduce the injury caused by the epileptic seizure evoked by PTZ.

In order to better study the protective effect of multiple OXC administrations, we used immunohistochemical procedures with anti-neurofilament and anti-beta tubulin as markers of mature neurons; their expression levels are altered in pathological conditions (Fig. 6).

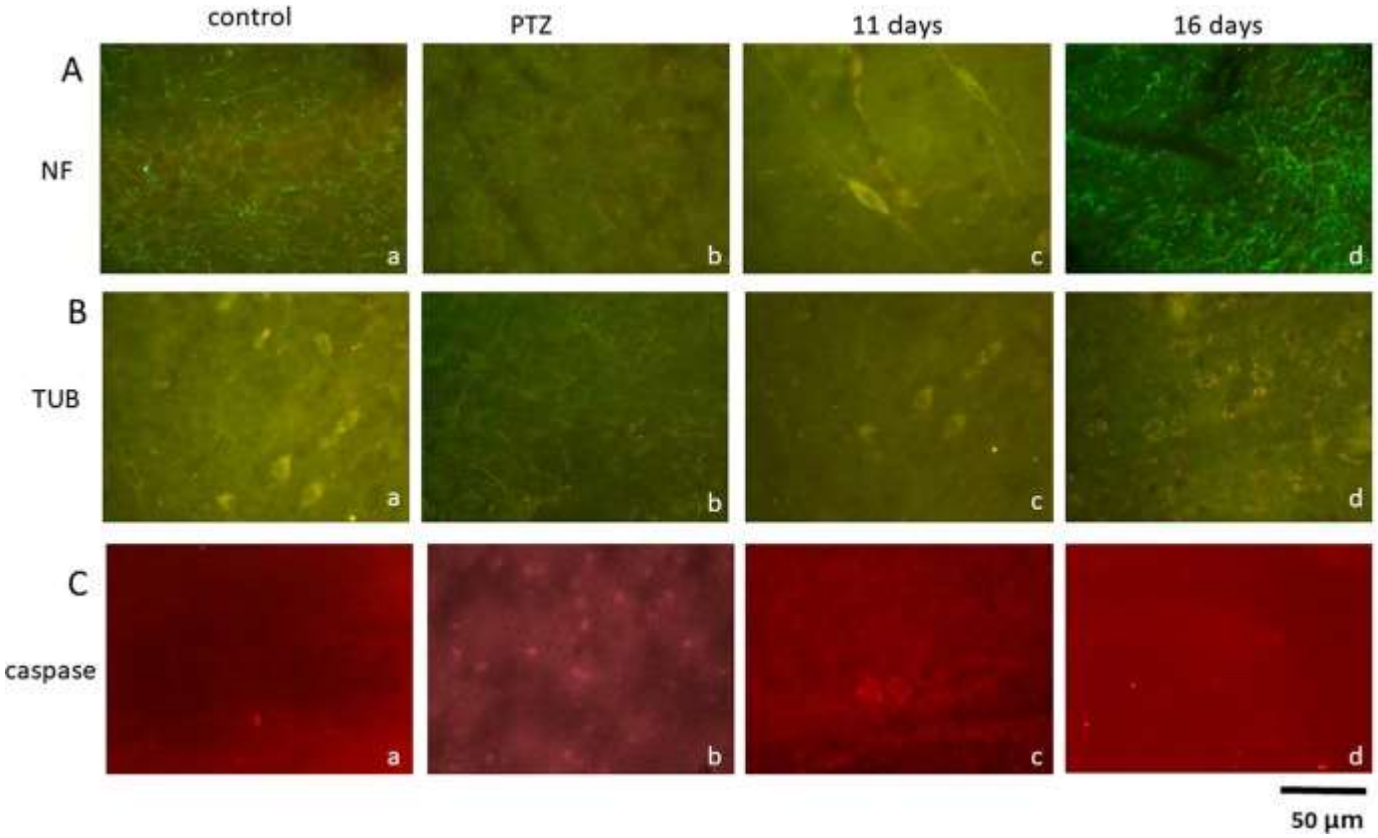

Fig. 6. Photomicrographs illustrating the expression of different markers in the hippocampus of non-treated rats (control) and treated with PTZ or PTZ-OXC loaded PLGA NPs for 11 and 16 days. The markers utilized were: anti-neurofilament (NF; A a–d), anti-beta tubulin (TUB; B a–d) as markers of mature neurons, visualized with Cy3 anti-rabbit antibody; anti-caspase3 (C a–d) as apoptotic cell death marker, visualized with goat anti-rabbit antibody IgG Fluorescein Isothiocyanate (FITC) Scale bar = 50 µm.

As shown in Fig. 6A and 6B the expression levels of both NF and TUB were reduced after PTZ injection (Fig. 6Ab and Bb) compared with controls (Fig. 6Aa and Ba). The expression levels of both neural markers were progressively increased in the rats pretreated with OXC for 11 (Fig. 6Ac for NF and Bc for TUB) and 16 (Fig. 6Ad for NF and Bd for TUB) days.

To verify apoptotic cell death we used immunohistochemical procedures with anti-caspase3 (Fig. 6C). We observed an increased expression level of caspase-3 in the rats injected with PTZ (Fig. 6Cb), compared with controls (Fig. 6Ca); whereas a decreased expression level of caspase-3 was shown in rats pre-treated with OXC for 11 (Fig. 6Cc) and 16 (Fig. 6Cd) days. These findings suggest a significant protection after chronic OXC loaded PLGA NP treatment in rats.

Our hypothesis is that a prevalent direct access of OXC (free or loaded NPs) into the brain through the nose is possible; based on our results we cannot exclude the involvement of other pathways.

4. Conclusions

In this study, a long-term storage of OXC encapsulated in biodegradable and biocompatible PLGA NPs was obtained. The re-suspended and cryo-protected OXC-loaded PLGA NPs were monodispersed with an average particle size < 300 nm and a PDI < 0.3, negative zeta potential with fair encapsulation efficiency values, around 85%. DSC, in accordance with FT-IR measurements,

demonstrated the amorphous form of the drug in the nanoformulations and its incorporation within the polymeric matrix.

Translocation of fluorescent DiR loaded NPs was assessed through FMT, and repeated IN administrations showed an increase of fluorescence in the brain of rodants. We used the RCS scale to evaluate the control of epileptic seizures in rats when free OXC was intranasally administrated, at different doses, thus producing a dose-response curve. The optimal (efficacy) dose of 0.5 mg/kg was selected to carry out the pharmacokinetic study. We showed that no free OXC amounts were detected in the CSF at 180 min after IV administration of the drug, while IN administration produced quantifiable amounts of OXC in the CSF of the rats, with relatively low concentrations. These studies revealed that free OXC (0.5 mg/kg) induced some protective effects against seizures but to achieve this result 3 administrations every 20 min were required (3 doses). These results suggest a direct nose to brain transfer of OXC because of its rapid appearance in the CSF and its simultaneous absence in the bloodstream. Our findings encourage the use of nano-based PLGA controlled release formulations to increase brain drug bioavailability.

Therefore, IN administration and OXC loaded PLGA NPs represent a combined strategy useful to control seizures, bypassing the BBB, increasing drug bioavailability in the brain and thus representing an alternative and high compliance administration route.

Conflict of interest

The author declare no conflict of interest.

Acknowledgements

Dr. Angela Bonaccorso was supported by the International Ph.D. program in Neuroscience, University of Catania, Italy. This work was supported by the Italian Ministry of University and Research (Prin 2010_H834LS). We wish to thank the Scientific Bureau of the University of Catania for language support.

Appendix A. Supplementary material

The following are the Supplementary data to this article:

Download : Download Word document (327KB)

Supplementary Data 1.

References

[1]

P.E.M. Smith
Clinical recommendations for oxcarbazepine
Seizure, 10 (2) (2001), pp. 87-91

[2]

R. Clinckers, I. Smolders, Y. Michotte, G. Ebinger, M. Danhof, R.A. Voskuyl, O. Della Pasqua
Impact of efflux transporters and of seizures on the pharmacokinetics of oxcarbazepine metabolite in the rat brain
Br. J. Pharmacol., 155 (7) (2008), pp. 1127-1138

[3]
M. Baulac, H. De Boer, C. Elger, M. Glynn, R. Kälviäinen, A. Little, J. Mifsud, E. Perucca, A. Pitkänen, P. Ryvlin
Epilepsy priorities in Europe: a report of the ILAE-IBE Epilepsy Advocacy Europe Task Force
Epilepsia, 56 (11) (2015), pp. 1687-1695

[4]
M. Bialer
Chemical properties of antiepileptic drugs (AEDs)
Adv. Drug Deliv. Rev., 64 (10) (2012), pp. 887-895

[5]
R. Moavero, M.E. Santarone, C. Galasso, P. Curatolo
Cognitive and behavioral effects of new antiepileptic drugs in pediatric epilepsy
Brain Dev., 39 (6) (2017), pp. 464-469

[6]
G.M. El-Zaafarany, M.E. Soliman, S. Mansour, G.A.S. Awad
Identifying lipidic emulsomes for improved oxcarbazepine brain targeting: in vitro and rat in vivo studies
Int. J. Pharm., 503 (1–2) (2016), pp. 127-140

[7]
P.G. Djupesland, J.C. Messina, R.A. Mahmoud
Therapeutic delivery
Ther. Deliv., 5 (12) (2014), pp. 1297-1314

[8]
M. Kapoor, J.C. Cloyd, R.A. Siegel
A review of intranasal formulations for the treatment of seizure emergencies
J. Control. Release, 237 (2016), pp. 147-159

[9]
L. Illum
Nasal drug delivery - recent developments and future prospects
J. Control. Release, 161 (2) (2012), pp. 254-263

[10]
G. Tosi, T. Musumeci, B. Ruozi, C. Carbone, D. Belletti, R. Pignatello, M.A. Vandelli, G. Puglisi

The 'fate' of polymeric and lipid nanoparticles for brain delivery and targeting: strategies and mechanism of blood-brain barrier crossing and trafficking into the central nervous system
J. Drug Deliv. Sci. Technol., 32 (2016)

[11]
M.D. Shadab, R.A. Khan, G. Mustafa, K. Chuttani, S. Baboota, J.K. Sahni, J. Ali
Bromocriptine loaded chitosan nanoparticles intended for direct nose to brain delivery: pharmacodynamic, pharmacokinetic and scintigraphy study in mice model
Eur. J. Pharm. Sci., 48 (3) (2013), pp. 393-405

[12]
D. Sharma, D. Maheshwari, G. Philip, R. Rana, S. Bhatia, M. Singh, R. Gabrani, S.K. Sharma, J. Ali, R.K. Sharma, S. Dang
Formulation and optimization of polymeric nanoparticles for intranasal delivery of lorazepam using Box-Behnken design: in vitro and in vivo evaluation
Biomed Res. Int., 2014 (2014)

[13]
A. Bonaccorso, T. Musumeci, M.F. Serapide, R. Pellitteri, I.F. Uchegbu, G. Puglisi
Nose to brain delivery in rats: effect of surface charge of rhodamine B labeled nanocarriers on brain subregion localization
Colloids Surf. B Biointerf., 154 (2017)

[14]
T. Musumeci, C. Bucolo, C. Carbone, R. Pignatello, F. Drago, G. Puglisi
Polymeric nanoparticles augment the ocular hypotensive effect of melatonin in rabbits
Int. J. Pharm., 440 (2) (2013), pp. 135-140
Article

[15]
K.O. Vasquez, C. Casavant, J.D. Peterson
Quantitative whole body biodistribution of fluorescent-labeled agents by non-invasive tomographic imaging
PLoS One, 6 (6) (2011)

[16]
M.P. van den Berg, S.G. Romeijn, J.C. Verhoef, F.W. Merkus
Serial cerebrospinal fluid sampling in a rat model to study drug uptake from the nasal cavity
J Neurosci Methods, 116 (1) (2002), pp. 99-107

[17]
H. Davson, K. Welch, M.B. Segal, The secretion of the cerebrospinal fluid, in: Anon. Physiol. Pathophysiol. Cerebrospinal Fluid, 1987, pp. 189–246.

[18]
J.L. MeeK, N.H. Neff
Is cerebrospinal fluid the major avenue for the removal of 5-hydroxyindoleacetic acid from the brain?

Neuropharmacology, 12 (1973), pp. 497-499

[19]
A. Madu, C. Cioffe, U. Mian, M. Burroughs, E. Tuomanen, M. Mayers, E. Schwartz, M. Miller
Pharmacokinetics of fluconazole in cerebrospinal fluid and serum of rabbits: Validation of an animal model used to measure drug concentrations in cerebrospinal fluid
Antimicrob. Agents Chemother., 38 (9) (1994), pp. 2111-2115

[20]
B.S. Haggag, A.H. Hasanin, M.H. Raafat, H.S. Abdel Kawy
Lamotrigine decreased hippocampal damage and improved vascular risk markers in a rat model of pentylenetetrazole induced kindling seizure
Korean J. Physiol. Pharmacol., 18 (3) (2014), pp. 269-278

[21]
A.M. Dyer, M. Hinchcliffe, P. Watts, J. Castile, I. Jabbal-Gill, R. Nankervis, A. Smith, L. Illum
Nasal delivery of insulin using novel chitosan based formulations: a comparative study in two animal models between simple chitosan formulations and chitosan nanoparticles
Pharm. Res., 19 (7) (2002), pp. 998-1008

[22]
S. Sharma, A. Parmar, S. Kori, R. Sandhir
PLGA-based nanoparticles: a new paradigm in biomedical applications
TrAC - Trends Anal. Chem., 80 (2016), pp. 30-40

[23]
M. Van Woensel, N. Wauthoz, R. Rosière, V. Mathieu, R. Kiss, F. Lefranc, B. Steelant, E. Dilissen, S.W. Van Gool, T. Mathivet, H. Gerhardt, K. Amighi, S. De Vleeschouwer
Development of siRNA-loaded chitosan nanoparticles targeting Galectin-1 for the treatment of glioblastoma multiforme via intranasal administration
J. Control. Release, 227 (2016), pp. 71-81

[24]
F. Ramazani, W. Chen, C.F. Van Nostrum, G. Storm, F. Kiessling, T. Lammers, W.E. Hennink, R.J. Kok
Strategies for encapsulation of small hydrophilic and amphiphilic drugs in PLGA microspheres: state-of-the-art and challenges
Int. J. Pharm., 499 (1–2) (2016), pp. 358-367

[25]
A. Bonaccorso, T. Musumeci, C. Carbone, L. Vicari, M.R. Lauro, G. Puglisi
Revisiting the role of sucrose in PLGA-PEG nanocarrier for potential intranasal delivery
Pharm. Dev. Technol. (2017)

[26]
Q. Liu, Y. Shen, J. Chen, X. Gao, C. Feng, L. Wang, Q. Zhang, X. Jiang
Nose-to-brain transport pathways of wheat germ agglutinin conjugated PEG-PLA nanoparticles
Pharm. Res., 29 (2) (2012), pp. 546-558

[27]
E. Ahmad, Y. Feng, J. Qi, W. Fan, Y. Ma, H. He, F. Xia, X. Dong, W. Zhao, Y. Lu, W. Wu
Evidence of nose-to-brain delivery of nanoemulsions: cargoes but not vehicles
Nanoscale, 9 (3) (2017), pp. 1174-1183

[28]
G. Rassu, E. Soddu, M. Cossu, A. Brundu, G. Cerri, N. Marchetti, L. Ferraro, R.F. Regan, P. Giunchedi, E. Gavini, A. Dalpiaz
Solid microparticles based on chitosan or methyl-β-cyclodextrin: a first formulative approach to increase the nose-to-brain transport of deferoxamine mesylate
J. Control. Release, 201 (Mar. 2015), pp. 68-77
Article

[29]
A. Mistry, S.Z. Glud, J. Kjems, J. Randel, K.A. Howard, S. Stolnik, L. Illum
Effect of physicochemical properties on intranasal nanoparticle transit into murine olfactory epithelium
J. Drug Target., 17 (7) (2009), pp. 543-552

[30]
A. Mistry, S. Stolnik, L. Illum
Nanoparticles for direct nose-to-brain delivery of drugs
Int. J. Pharm., 379 (1–2) (2009), pp. 146-157
Article

[31]
W. Abdelwahed, G. Degobert, S. Stainmesse, H. Fessi
Freeze-drying of nanoparticles: formulation, process and storage considerations
Adv. Drug Deliv. Rev., 58 (15) (Dec. 2006), pp. 1688-1713
Article

[32]
T. Musumeci, R. Pignatello
Reduce the gap from bench to bedside for nanomedicines increasing the stability to long-term storage
Biomaterials – Physics and Chemistry – New Edition, INTECH OPEN, London (2018), pp. 1-7

[33]
A. Mistry, S. Stolnik, L. Illum
Nose-to-brain delivery: investigation of the transport of nanoparticles with different surface characteristics and sizes in excised porcine olfactory epithelium
Mol. Pharm., 12 (8) (2015), pp. 2755-2766

[34]
T. Musumeci, L. Vicari, C.A. Ventura, M. Gulisano, R. Pignatello, G. Puglisi
Lyoprotected nanosphere formulations for paclitaxel controlled delivery
J. Nanosci. Nanotechnol., 6 (9–10) (2006)

[35]
M. Stevanović, A. Radulović, B. Jordović, D. Uskoković
Poly(DL-lactide-co-glycolide) nanospheres for the sustained release of folic acid
J. Biomed. Nanotechnol., 4 (2008), pp. 1-10

[36]
H. Koradia, S. Butani, M. Gohel
Studies in oxcarbazepine microspheres employing Plackett and Burman design
Int. J. Pharm. Pharm. Sci., 6 (7) (2014), pp. 305-310

[37]
K.M. Lutker, A.J. Matzger
Crystal polymorphism in a carbamazepine derivative: oxcarbazepine
J. Pharm. Sci., 99 (2) (2010), pp. 794-803
Article

[38]
A. Lopalco, H. Ali, N. Denora, E. Rytting
Oxcarbazepine-loaded polymeric nanoparticles: Development and permeability studies across in vitro models of the blood–brain barrier and human placental trophoblast
Int. J. Nanomed., 10 (2015), pp. 1985-1996

[39]
R. Dal Magro, F. Ornaghi, I. Cambianica, S. Beretta, F. Re, C. Musicanti, R. Rigolio, E. Donzelli, A. Canta, E. Ballarini, G. Cavaletti, P. Gasco, G. Sancini
ApoE-modified solid lipid nanoparticles: a feasible strategy to cross the blood-brain barrier
J. Control. Release, 249 (Mar. 2017), pp. 103-110
Article

[40]
R. Dal Magro, B. Albertini, S. Beretta, R. Rigolio, E. Donzelli, A. Chiorazzi, M. Ricci, P. Blasi, G. Sancini
Artificial apolipoprotein corona enables nanoparticle brain targeting
Nanomed. Nanotechnol. Biol. Med., 14 (2) (2018), pp. 429-438

[41]
A. Fortuna, G. Alves, A. Serralheiro, J. Sousa, A. Falcão
Intranasal delivery of systemic-acting drugs: small-molecules and biomacromolecules
Eur. J. Pharm. Biopharm., 88 (1) (2014), pp. 8-27

[42]
D. Hainzl, A. Parada, P. Soares-da-Silva

Metabolism of two new antiepileptic drugs and their principal metabolites S (+)- and R(−)-10,11-dihydro-10-hydroxy carbamazepine
Epilepsy Res., 44 (2–3) (2001), pp. 197-206

[43]
W.M. Pardridge
Drug transport across the blood-brain barrier
J. Cereb. Blood Flow Metab., 32 (11) (2012), pp. 1959-1972

[44]
R. Clinckers, I. Smolders, A. Meurs, G. Ebinger, Y. Michotte
Quantitative in vivo microdialysis study on the influence of multidrug transporters on the blood-brain barrier passage of oxcarbazepine: concomitant use of hippocampal monoamines as pharmacodynamic markers for the anticonvulsant activity
J. Pharmacol. Exp. Ther., 314 (2) (2005), pp. 725-731

[45]
T.W. May, E. Korn-Merker, B. Rambeck
Clinical pharmacokinetics of oxcarbazepine
Clin. Pharmacokinet., 42 (12) (2003), pp. 1023-1042